Implementing Orthogonal Binary Overlay on a Pulse Train using Frequency Modulation

As reported recently, overlaying orthogonal phase coding on any coherent train of identical radar pulses, removes most of the autocorrelation near sidelobes and lowers the recurrent lobes. The present work shows that both properties are maintained when a binary orthogonal overlay is replaced by its "derivative phase" (DP) frequency modulation (FM) equivalent. Frequency modulated overlay is more spectrum efficient and would be easier to implement when the original pulses are already frequency modulated.

I. INTRODUCTION

Achieving Doppler resolution in radar usually requires a coherent train of P pulses. In most cases the train is constructed by repeating the same compressed pulse. It was recently reported [1–3] that overlaying the P identical pulses with an orthogonal set of P sequences, each one constructed of M elements, will remove completely the sidelobes of the autocorrelation function (ACF) over the delay range $t_s \le \tau \le T$, where t_s is the duration of one element of the sequence, which is referred to as a slice, and $T = Mt_s$ is the pulse duration. In [1], [2] and [3] the orthogonal set was implemented using phase modulation. The penalty for adding phase modulation is spectrum broadening, typical of conventional phase coding. One method to reduce the spectral width of phase coded radar signals, while maintaining constant envelope, is the "derivative phase (DP) modulation" [4, 5]. We apply this method, instead of the phase-coded orthogonal overlay, and check the resulting ACF and spectrum.

Subsections A and B of the introduction briefly describe the orthogonal overlay concept and the derivative phase (DP) method. In the following sections examples are given of using DP overlay on four different pulse compression signals.

A. Orthogonal Overlay

In [1], [2], and [3] the orthogonal set was implemented using phase modulation. An example of a P-by-M binary orthogonal set, where $P = M = 8$, can be described starting with the phase matrix

$$\varphi = \{\varphi_{p,m}\} = \pi \begin{bmatrix} 0 & 0 & 0 & 0 & 0 & 0 & 0 & 0 \\ 0 & 0 & 1 & 1 & 1 & 1 & 0 & 0 \\ 0 & 1 & 1 & 0 & 0 & 1 & 1 & 0 \\ 0 & 0 & 0 & 0 & 1 & 1 & 1 & 1 \\ 0 & 1 & 0 & 1 & 0 & 1 & 0 & 1 \\ 0 & 0 & 1 & 1 & 0 & 0 & 1 & 1 \\ 0 & 1 & 0 & 1 & 1 & 0 & 1 & 0 \\ 0 & 1 & 1 & 0 & 1 & 0 & 0 & 1 \end{bmatrix}. \quad (1)$$

The actual orthogonal set is given by the matrix

$$\mathbf{A} = \{a_{p,m}\} = \{\exp(j\varphi_{p,m})\}. \quad (2)$$

Clearly, the elements of $\mathbf{A}$ get only two values: $+1$ and -1. Polyphase orthogonal sets were also described in [1], [2], and [3] but they are not relevant to the present paper. Recall that the matrix $\mathbf{A}$ is said to be orthogonal when the dot product between any two columns of $\mathbf{A}$ is zero, implying that the matrix $\mathbf{A}^T\mathbf{A}$ is diagonal. Note also that orthogonal P-by-M matrices $\mathbf{A}$ exist only for $M \le P$. The overlay is implemented by phase modulating the pth pulse by the pth row of $\mathbf{A}$.

One problem caused by adding a binary phase-coded overlay, is the broadening of the spectrum. An example is given using a train of 8 constant frequency (i.e., unmodulated) pulses, with and without binary overlay. The relationships between the slice width t_s, the pulsewidth T, the pulse repetition interval T_r and the total signal duration PT_r are

$$T = Mt_s = 8t_s$$
$$T_r = 2.5T = 20t_s$$
$$PT_r = 8T_r = 160t_s.$$

The large duty cycle ($T/T_r = 0.4$) was selected in order to simplify the drawings. Fig. 1 presents the well-known ACF and magnitude spectrum of a coherent train of 8 unmodulated pulses. The spectrum's first local null is at $fPT_r = 1$, with a major null at $f = 1/T$, namely at $fPT_r = 20$. Adding binary phase modulation with a slice width equal to $t_s = T/8$ should broaden the spectrum by a factor of 8. Thus the first null is found at $fPT_r = 160$ (see Fig. 2, middle subplot). Because of the instant phase transition at slice boundary, the spectrum exhibits an extended skirt, decaying at a rate of 6 dB/octave, as seen in the bottom subplot of Fig. 2. Comparing the autocorrelation (top subplots) in Figs. 1 and 2, demonstrates how adding the orthogonal overlay removed the near-sidelobes over $t_s \le \tau \le T = 8t_s$, and lowered the recurrent lobes around multiples of T_r, namely multiples of $20t_s$.

Manuscript received June 17, 2004; revised September 27, 2004; released for publication October 29, 2004.

IEEE Log No. T-AES/41/1/844832.

Refereeing of this contribution was handled by E. S. Chornoboy.

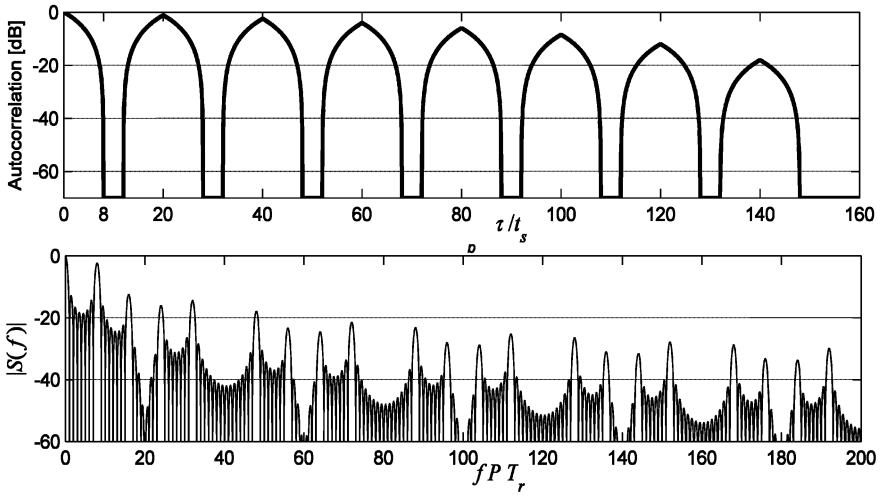

Fig. 1. ACF (top) and spectrum (bottom) of train of 8 constant frequency pulses (without overlay).

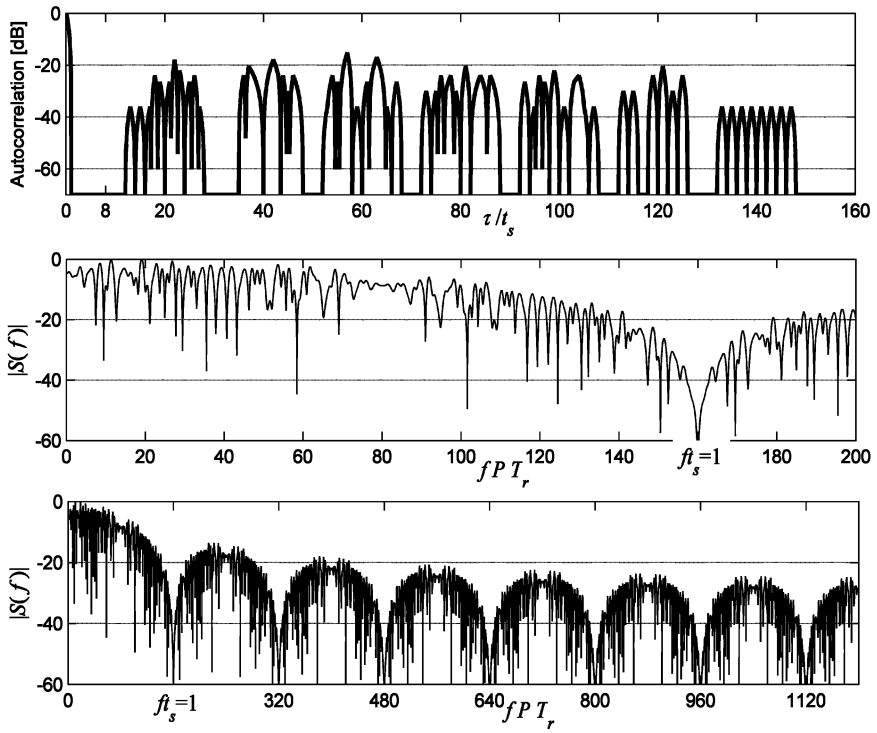

Fig. 2. ACF (top) and spectrum (middle and bottom) of train of 8 constant frequency pulses (with orthogonal phase-coded overlay).

B. Derivative Phase Modulation

DP modulation [4, 5] differs from conventional binary phase modulation by replacing phase jumps with phase slopes (frequency steps). The frequency steps are so designed that at the end of the slice duration t_s the accumulated phase change is the desired 0 or π. Zero phase accumulation is obtained by splitting the slice into two bits $t_s = 2t_b$; during the first bit the frequency step is $\Delta f = 1/4t_b$ yielding accumulated phase of $2\pi\Delta f t_b = \pi/2$; during the second bit the frequency step is $-\Delta f$ yielding accumulated phase of $-\pi/2$; hence, zero total phase accumulation during a slice. Phase accumulation of π (or $-\pi$) is achieved by maintaining the frequency step of $-\Delta f$ during the entire slice.

There are several variations to DP. In the one to be used here the split slice, in which the frequency modulation (FM) is $\{\Delta f, -\Delta f\}$, is used in the first slice of a sequence, and whenever the current slice is identical to the previous slice. A $\{-\Delta f, -\Delta f\}$ FM is used when the current slice is different from the previous slice. Equation (3) presents the FM matrix corresponding to the orthogonal phase-coded matrix

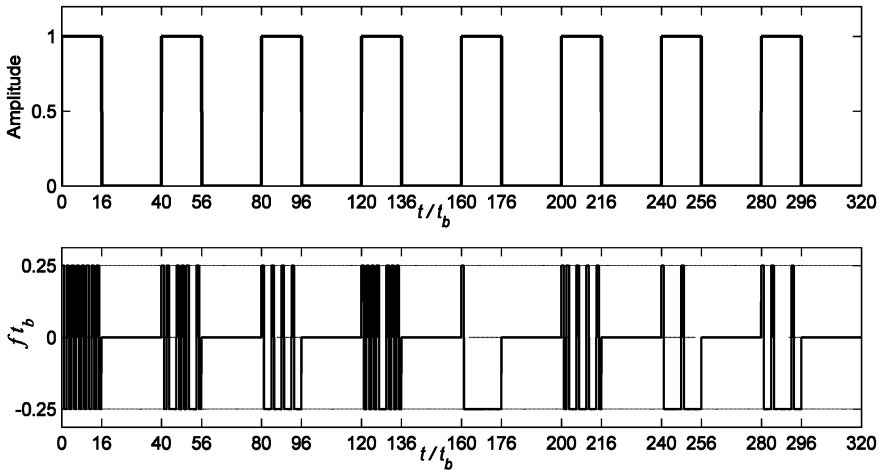

Fig. 3. Amplitude (top) and frequency (bottom) of train of 8 constant frequency pulses (with derivative phase overlay).

in (1)

$$\mathbf{F} = \Delta f \begin{bmatrix} 1 & -1 & 1 & -1 & 1 & -1 & 1 & -1 & 1 & -1 & 1 & -1 & 1 & -1 & 1 & -1 \\ 1 & -1 & 1 & -1 & -1 & -1 & 1 & -1 & 1 & -1 & 1 & -1 & -1 & -1 & 1 & -1 \\ 1 & -1 & -1 & -1 & 1 & -1 & -1 & -1 & 1 & -1 & -1 & -1 & 1 & -1 & -1 & -1 \\ 1 & -1 & 1 & -1 & 1 & -1 & 1 & -1 & -1 & -1 & 1 & -1 & 1 & -1 & 1 & -1 \\ 1 & -1 & -1 & -1 & -1 & -1 & -1 & -1 & -1 & -1 & -1 & -1 & -1 & -1 & -1 & -1 \\ 1 & -1 & 1 & -1 & -1 & -1 & 1 & -1 & -1 & -1 & 1 & -1 & -1 & -1 & 1 & -1 \\ 1 & -1 & -1 & -1 & -1 & -1 & -1 & -1 & 1 & -1 & -1 & -1 & -1 & -1 & -1 & -1 \\ 1 & -1 & -1 & -1 & 1 & -1 & -1 & -1 & -1 & -1 & -1 & -1 & 1 & -1 & -1 & -1 \end{bmatrix}. \tag{3}$$

Note that there are 92 "−1" in (3) and only 36 "+1". This implies that the spectrum of the complex envelope of the signal containing this type of overlay will be shifted downward in frequency. This is demonstrated in Fig. 5. Another FM matrix that corresponds to the PONS [3, 6] orthogonal matrix is given in (4). The frequency coding in (3) is used henceforth, unless stated otherwise. The two frequency coding overlays yield exactly the same ACF over the delay span $|\tau| \leq T$, but the ambiguity functions over that span differ at non-zero Doppler shifts. The recurrent lobes of the ACFs are also affected by the specific frequency coding overlay

In the phase-coded overlay defined by (1) and (2), it was straightforward to show that the overlay (namely **A**) was orthogonal. In the frequency-coded overlay described by (3) or (4), the meaning of orthogonality is not so simple. The test will have to be the removal of the autocorrelation sidelobes.

Because the suggested new overlay involves FM, it is of special interest to test it with signals that are already frequency modulated. In Sections III, IV, and V it is applied to Costas, linear FM (LFM), and modified Costas. But first, in Section II, it is applied to unmodulated pulses, in order to compare

$$\mathbf{F} = \Delta f \begin{bmatrix} 1 & -1 & 1 & -1 & 1 & -1 & -1 & -1 & -1 & -1 & 1 & -1 & -1 & -1 & -1 & -1 \\ 1 & -1 & 1 & -1 & 1 & -1 & -1 & -1 & 1 & -1 & 1 & -1 & -1 & -1 & -1 & -1 \\ 1 & -1 & 1 & -1 & -1 & -1 & -1 & -1 & 1 & -1 & 1 & -1 & 1 & -1 & -1 & -1 \\ 1 & -1 & 1 & -1 & -1 & -1 & -1 & -1 & -1 & -1 & 1 & -1 & 1 & -1 & -1 & -1 \\ 1 & -1 & -1 & -1 & -1 & -1 & 1 & -1 & -1 & -1 & -1 & -1 & 1 & -1 & 1 & -1 \\ 1 & -1 & -1 & -1 & -1 & -1 & 1 & -1 & 1 & -1 & -1 & -1 & 1 & -1 & 1 & -1 \\ 1 & -1 & -1 & -1 & 1 & -1 & 1 & -1 & 1 & -1 & -1 & -1 & -1 & -1 & 1 & -1 \\ 1 & -1 & -1 & -1 & 1 & -1 & 1 & -1 & -1 & -1 & -1 & -1 & -1 & -1 & 1 & -1 \end{bmatrix}. \tag{4}$$

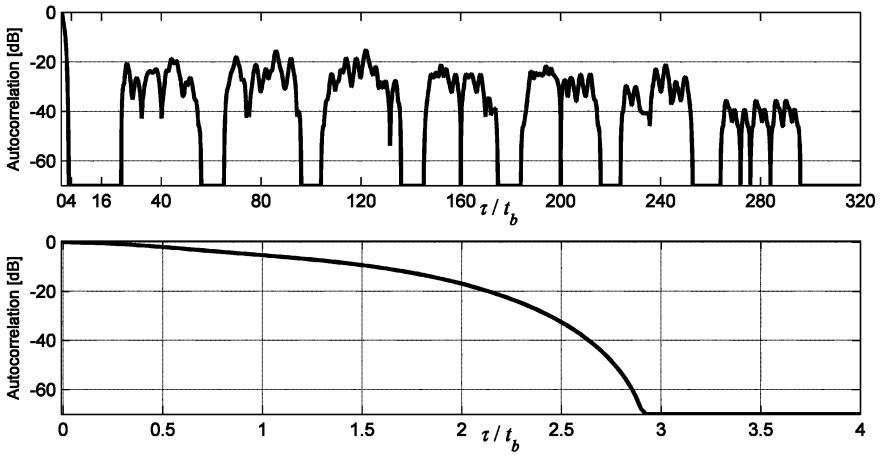

Fig. 4. ACF of train of 8 constant frequency pulses (with derivative phase overlay).

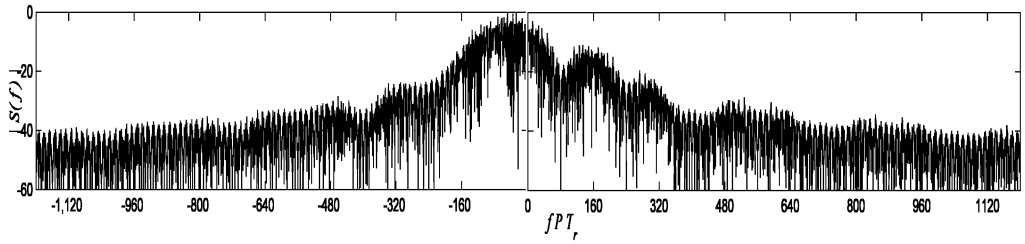

Fig. 5. Spectrum of train of 8 constant frequency pulses (with derivative phase overlay).

its performances with those obtained with phase-coded overlay and presented in Fig. 2.

II. DERIVATIVE PHASE OVERLAY ON UNMODULATED PULSES

The original pulse train to which the DP overlay is added is identical to the one used to generate Figs. 1 and 2. However, the basic time unit in the drawings is $t_b = t_s/2$, because t_b is the duration of each frequency step. The remaining relationships are

$$T = Mt_s = 2Mt_b = 16t_b$$
$$T_r = 2.5T = 40t_b$$
$$PT_r = 8T_r = 320t_b.$$

The signal's amplitude and frequency steps in the time domain are plotted in Fig. 3, the resulted ACF in Fig. 4, and the spectrum in Fig. 5.

The top subplot in Fig. 4 displays the entire ACF and should be compared with the top subplot of Fig. 2 (recalling that $t_s = 2t_b$). It shows that indeed most of the near sidelobes are removed. The zoom in the bottom subplot of Fig. 4 shows the extent of the ACF sidelobes removal. Here the sidelobes reach a level of -70 dB at $\tau = 2.8t_b = 1.4t_s$, and (not shown) become identically zero for $t \geq 3t_b = 1.5t_s$. Recall that in the phase-coded orthogonal overlay the ACF sidelobes became identically zero at $\tau = t_s$. The practical conclusion is that the DP overlay removes the near sidelobes almost as well as the phase-coded orthogonal overlay did. The attenuation of the ACF recurrent lobes is also very similar.

An important advantage of the DP overlay is the more confined spectrum, as can be seen by comparing Fig. 2 (bottom subplot) with Fig. 5. At normalized frequency of $fPT_r = 1200$ ($ft_s = 7.5$) the spectrum of the phase-coded overlay (Fig. 2) reached a level of approximately -25 dB, while the spectrum of the DP overlay was down to -40 dB. In Fig. 5 both negative and positive frequencies are displayed in order to show the asymmetrical spectrum.

Overlay on a train of unmodulated pulses provides an opportunity to show the effect of the particular overlay code on the ambiguity function. Fig. 6 presents the ambiguity functions (extended in delay for the duration of one pulse) using both types of frequency coding overlay matrices. The zero-Doppler cut of the ambiguity function confirms the removed ACF sidelobes. The plot shows the gradual build-up of sidelobes with increasing Doppler, slower with the PONS based overlay. The first Doppler null at $\tau = 0$ appears at a Doppler shift that is the inverse of the entire train duration, namely at $\nu = 1/PT_r$. This is expected, because the added FM does not affect the zero-delay cut of the ambiguity function.

It is worth noting that DP can't always replace binary phase coding. For example, if DP is used to create a complementary pair, the sidelobes are not necessarily completely removed. Consider the ACF

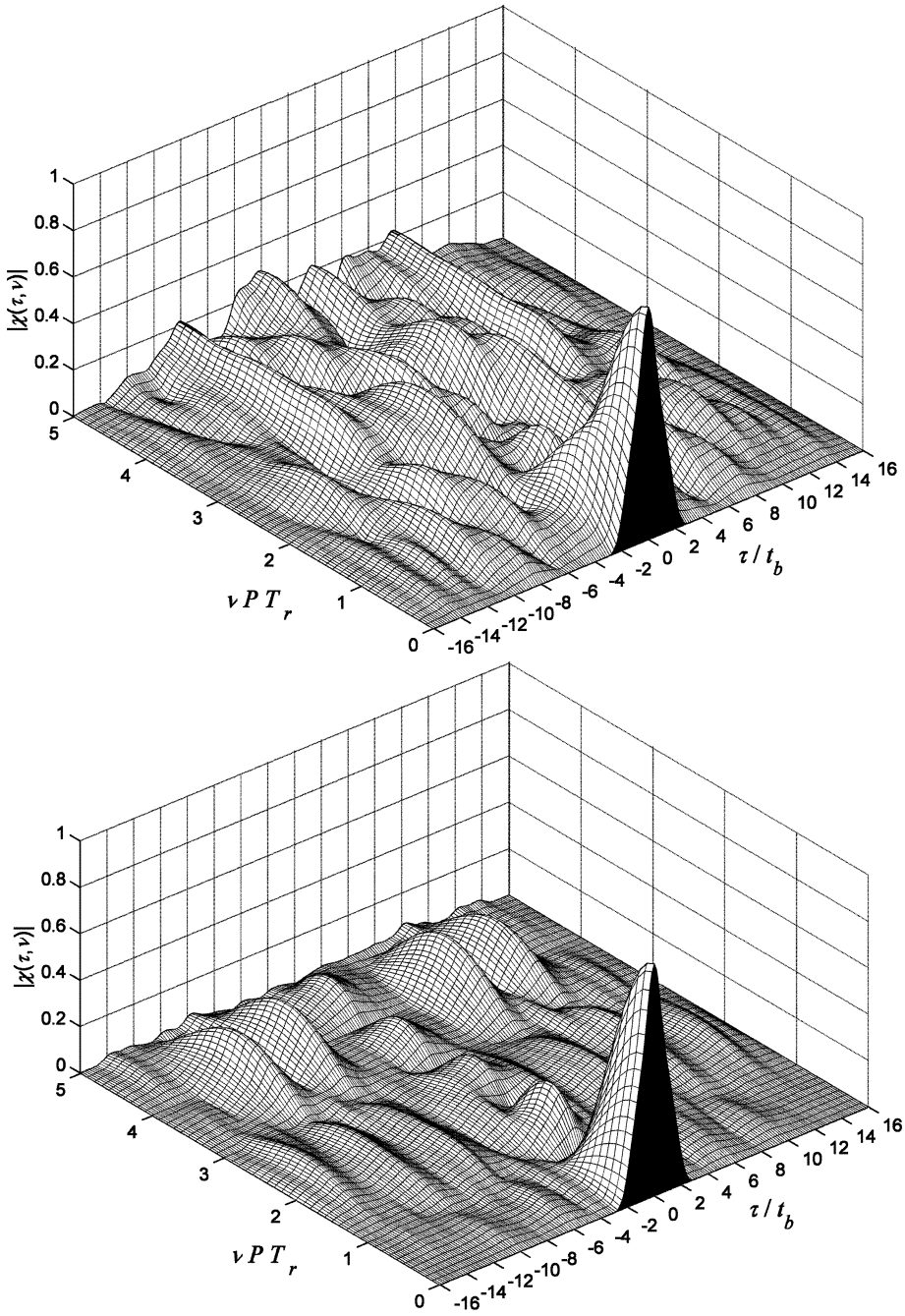

Fig. 6. Partial ambiguity function of train of 8 constant frequency pulses. DP overlay: top—using (3), bottom—using (4) (PONS). Delay axis extends as far as one pulse duration.

sidelobes of a 26 element complementary pair

[0	0	0	0	1	0	0	1	1	0	1	0	0	0	0	0	1	0	1	1	1	0	0	1	1	1]
[0	0	0	0	1	0	0	1	1	0	1	0	1	0	1	1	0	1	0	0	0	1	1	0	0	0].

As Fig. 7 shows, the ACF sidelobes remain at a level of approximately −35 dB for one half of the pulse duration, and becomes identically zero only for the remaining half.

DP modulation is similar in many respects to continuous phase frequency shift keying (CPFSK) used in communications [7], and in particular to minimum shift keying (MSK). In those methods

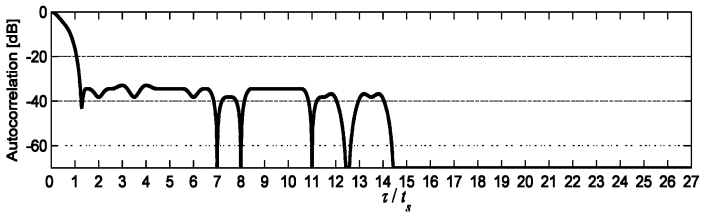

Fig. 7. ACF of 26 element binary complementary pair implemented using DP.

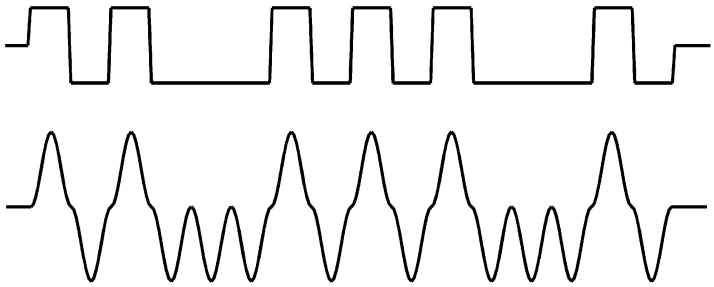

Fig. 8. Frequency evolution in 2nd pulse (out of 8 pulses) using rectangular (top) and raised-cosine (bottom) overlay waveforms.

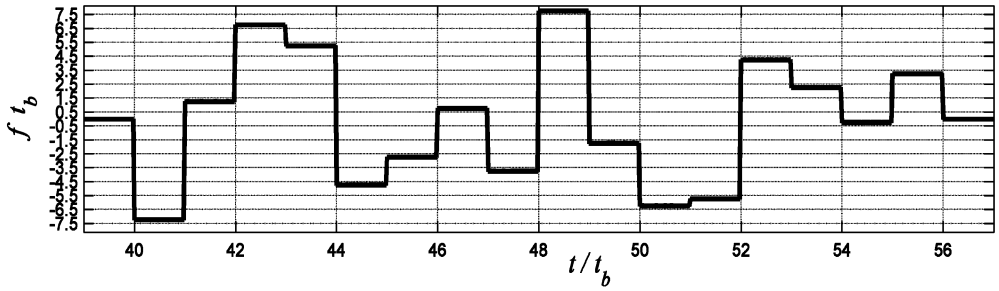

Fig. 9. Frequency evolution in 2nd 16-element Costas pulse (out of 8 pulses) (with DP overlay).

further reduction in the spectral width is obtained by replacing the rectangular frequency step with other waveforms, e.g., a raised-cosine (*RC*) waveform,

$$r(t) = 1 - \cos\frac{2\pi t}{t_b}, \qquad 0 \le t \le t_b. \tag{5}$$

We tested *RC* waveform instead of the rectangular frequency modulating waveform, through which the binary overlay was implemented. A comparison of the frequency evolution of the 2nd unmodulated (other than overlay) pulse, in both approaches is shown in Fig. 8. Note that the peak frequency deviation in the *RC* waveform (lower subplot) is twice the peak frequency deviation of the rectangular waveform, in order to achieve the same phase accumulation at the end of each bit. We found out that the *RC* waveform produced the same ACF sidelobe removal as did the rectangular waveform. However, there was no meaningful improvement in the spectrum. Hence, in the remaining sections, the rectangular waveform is used.

Having demonstrated, using a train of 8 unmodulated pulses, that the DP overlay is as effective, in removing ACF sidelobes, as orthogonal phase-coded binary overlay, we proceed to check its performances with three frequency modulated pulse trains: Costas, LFM, and modified Costas. In the case of the binary phase-coded overlay [1], it was shown that as far as removing the ACF sidelobes, the type of the underlying identical pulses made no difference. We thus expect that once we find a frequency-coded replacement to the binary overlay, as demonstrated on the unmodulated pulses, it will work just as well on modulated pulses, no matter what their particular modulation is.

III. DERIVATIVE PHASE OVERLAY ON COSTAS PULSES

The number of slices M in an orthogonal overlay need not match the number of elements in the original coded pulse. Still, it is appealing to match the two. Since there are 16 frequency steps in an 8 slice DP overlay, we choose a 16-element Costas pulse [8] with the frequency sequence: {1 10 15 14 4 6 9 5 16 7 2 3 13 11 8 12}. The coherent train still contains 8 pulses. The minimal frequency step in a Costas signal is $\Delta f_{\text{Costas}} = \pm 1/t_b$,

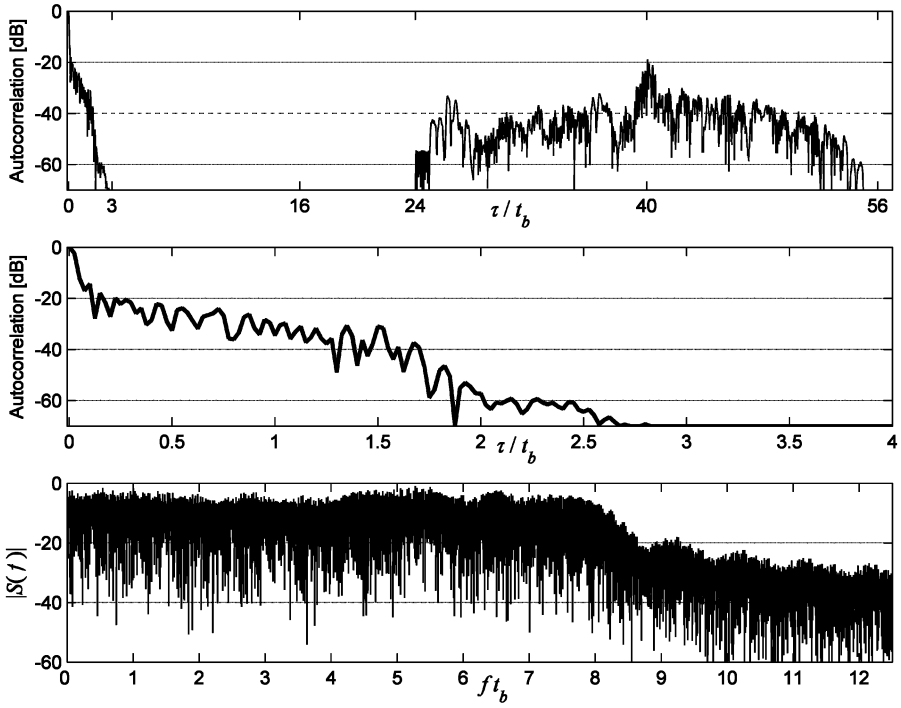

Fig. 10. ACF (top and middle) and spectrum (bottom) of train of eight 16-element Costas pulses (with DP overlay).

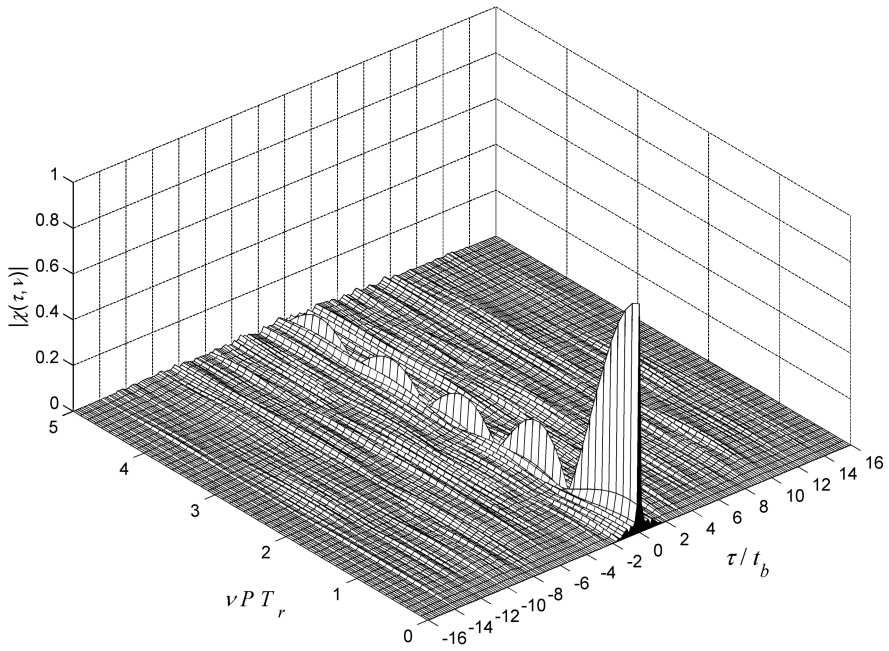

Fig. 11. Partial ambiguity function of train of eight 16-element Costas pulses (with DP overlay). Delay axis extended as far as one pulse duration.

while the overlay frequency steps are $\Delta f_{\text{overlay}} = \pm 1/4t_b$. Thus, the overlay adds relatively small changes to the original frequency steps. The frequency evolution of the second pulse in the train (after DP overlay) is plotted in Fig. 9. Without the overlay the frequency values would have been aligned with the vertical grid.

The resulting ACF and spectrum are plotted in Fig. 10. The top subplot presents the ACF on a delay scale extended as far as the first recurrent lobe. The middle subplot zooms on the near sidelobes. The removal of sidelobes for $\tau > 2.8t_b$ is evident. Comparing the middle subplot of Fig. 10 with the bottom subplot of Fig. 4 shows how much the wide bandwidth Costas signal narrows the ACF mainlobe. The pulse compression of a 16 element Costas signal is $16^2 = 256$. Indeed the mainlobe width is approximately $t_b/16 = T/256$. The lower subplot

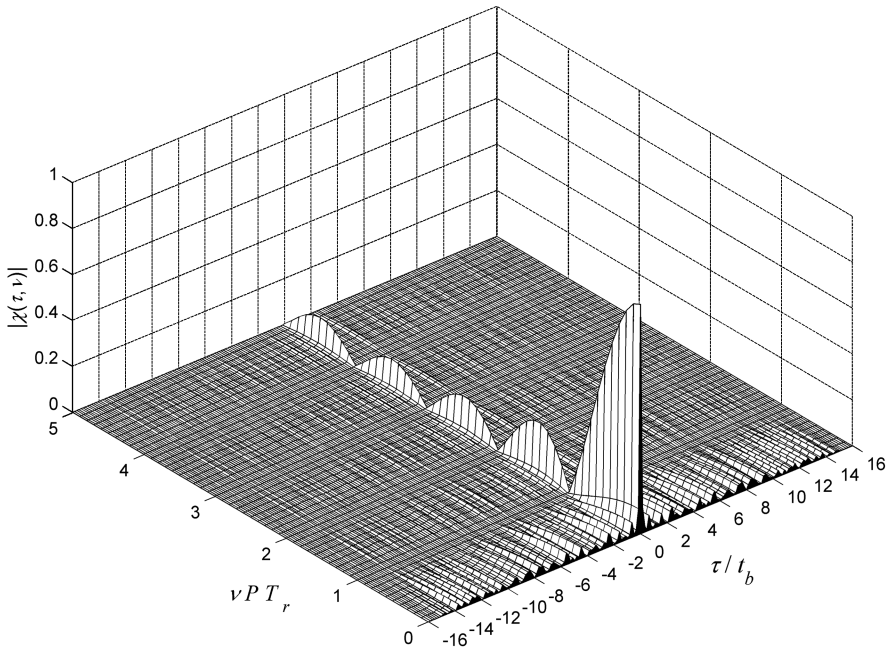

Fig. 12. Partial ambiguity function of train of eight 16-element Costas pulses (without overlay). Delay axis extended as far as one pulse duration.

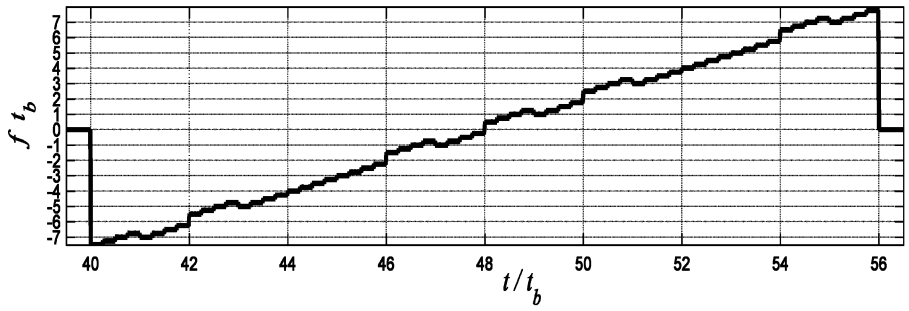

Fig. 13. Frequency evolution in 2nd LFM pulse (out of 8 pulses) (with DP overlay).

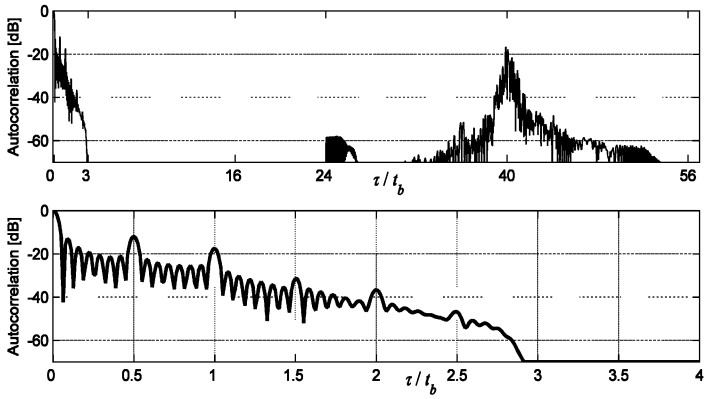

Fig. 14. ACF of train of eight LFM pulses (with DP overlay). Delay axis extended as far as: top—first recurrent lobe, bottom—1/4 pulse duration.

shows the relatively flat spectrum of the Costas signal, extending (in positive frequencies) up to $8/t_b$. The combined effect of narrow mainlobe (due to Costas) and removed zero-Doppler sidelobes (due to the overlay) is seen clearly in the ambiguity function (Fig. 11). For comparison the ambiguity function of the same Costas pulse train without an overlay is shown in Fig. 12. It seems incredible how the small frequency dither that the DP overlay adds to the Costas frequencies makes such a profound change in the ambiguity function sidelobe pattern near zero-Doppler.

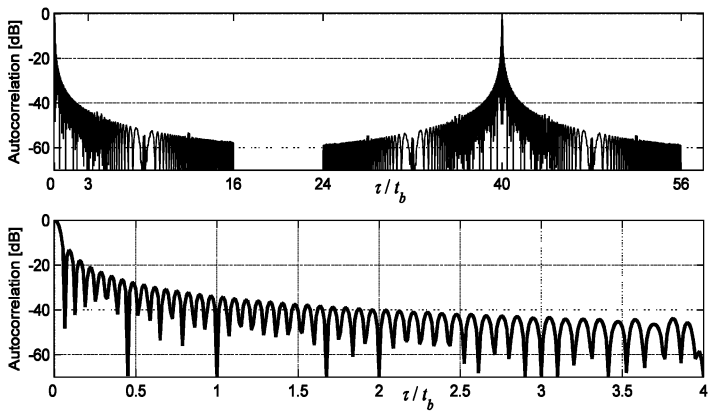

Fig. 15. ACF of train of eight LFM pulses (without overlay). Delay axis extended as far as: top—first recurrent lobe, bottom—1/4 pulse duration.

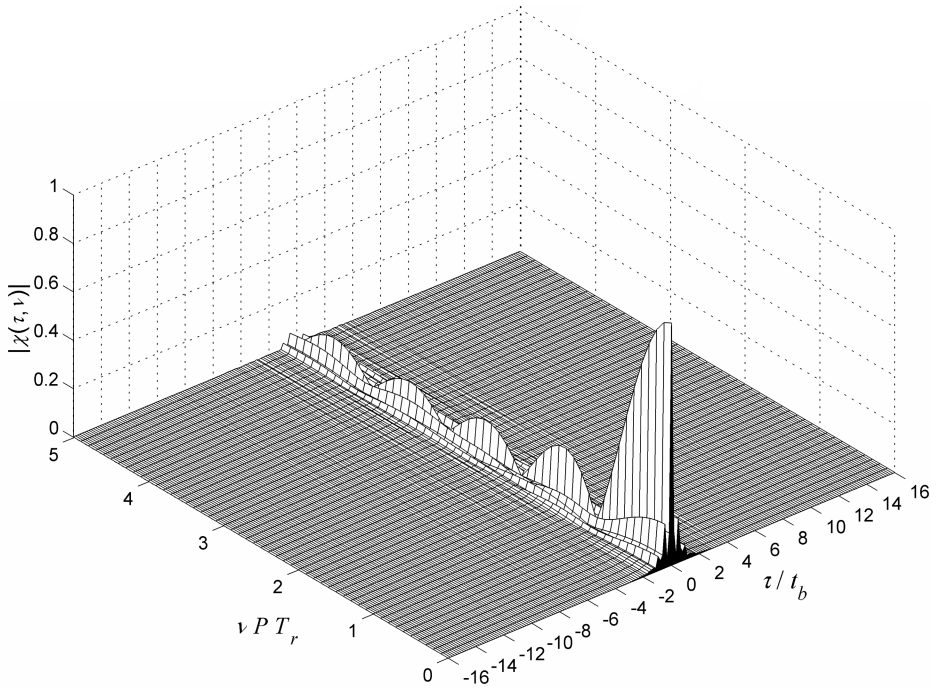

Fig. 16. Partial ambiguity function of train of eight LFM pulses (with DP overlay). Delay axis extended as far as one pulse duration.

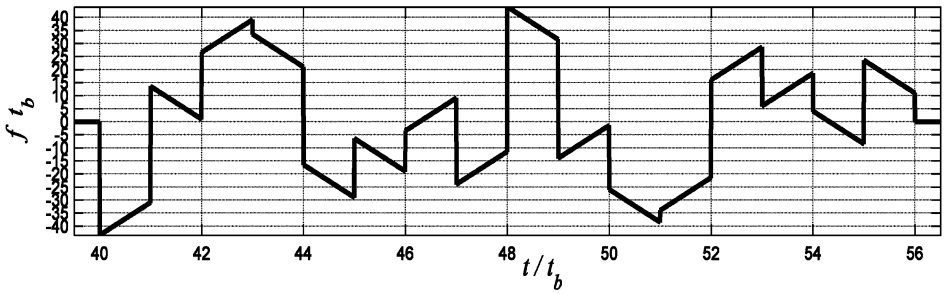

Fig. 17. Frequency evolution in 2nd 16-element modofied Costas pulse (out of 8 pulses) (with DP coding).

IV. DERIVATIVE PHASE OVERLAY ON LFM PULSES

Stepped LFM pulses are considered in this example. Two new parameters need to be introduced: the step duration t_c and the frequency step df. In order to obtain a similar bandwidth to the Costas example, we will choose $t_c = t_b/4$, $df = 1/16t_c$. The frequency evolution during the second pulse (out of 8 pulses) is shown in Fig. 13. The ACF appears in Fig. 14.

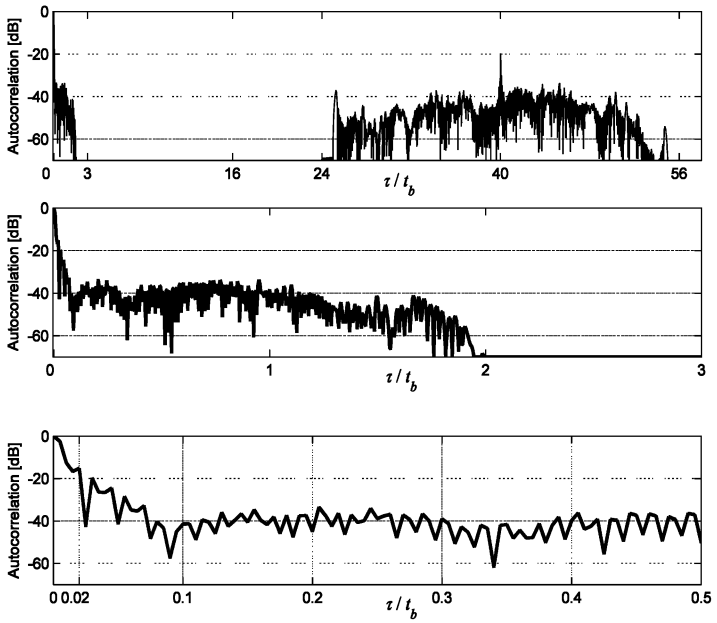

Fig. 18. ACF of train of eight modified Costas pulses (with DP overlay). Delay axis extended as far as: top—first recurrent lobe, middle—3/16 pulse duration, bottom—1/32 pulse duration.

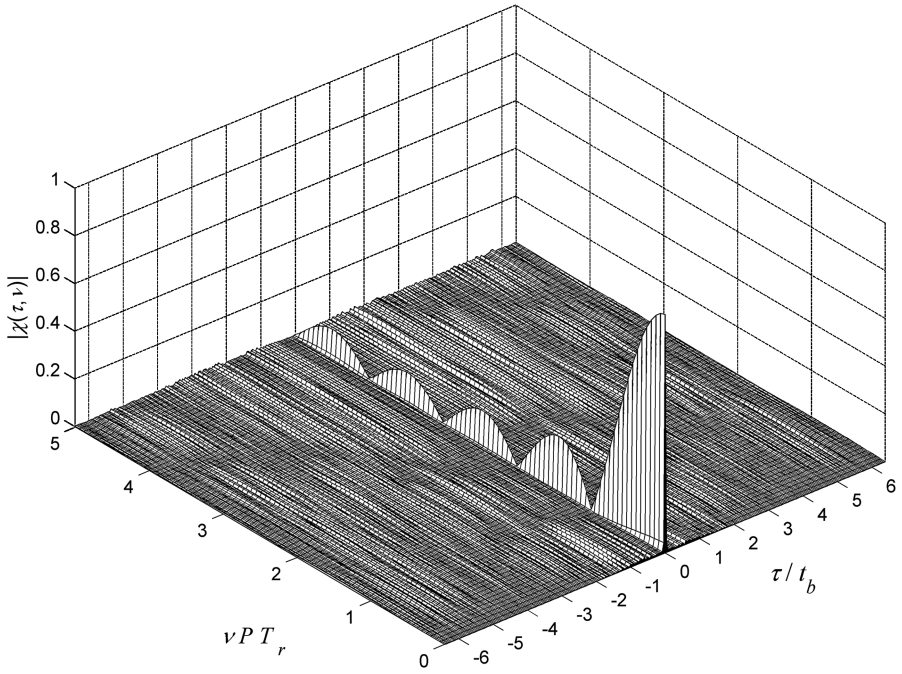

Fig. 19. Partial ambiguity function of train of eight 16-element modified Costas pulses (with DP overlay). Delay axis extended as far as 3/8 pulse duration.

Comparing Fig. 14 with the ACF of a train of identical LFM pulses without overlay (Fig. 15) reveals that indeed, with overlay, the sidelobes beyond $|\tau| > 3t_b$ were removed, and the recurrent lobe was reduced. However, most of the remaining sidelobes, over $|\tau| < 2t_b$, are higher than without overlay. In both Figs. 14 and 15 the first null of the ACF is at $t_b/16 = T/256$, as expected since the time bandwidth product is 256. Finally, Fig. 16 displays the ambiguity function of the LFM train with derivative phase overlay. It shows that the slice with sidelobes $|\tau| < 3t_b$ is actually a strip that extends to higher Doppler frequencies.

V. DERIVATIVE PHASE OVERLAY ON MODIFIED COSTAS PULSES

A modified Costas pulse [2, 3, 9] combines Costas frequency coding with LFM within each Costas element (bit). Adding LFM allows increasing the size of the frequency step beyond the nominal $\Delta f_{\text{Costas}} =$

$\pm 1/t_b$. The increased frequency step results in wider bandwidth, hence higher pulse compression. One of several discrete relationships must exist between the LFM bandwidth B, the bit duration t_b, and the increased frequency step $\Delta f_{\text{Mod. Costas}}$, in order to nullify the ACF grating lobes that would show up without the LFM. The polarity of the LFM slope need not be fixed. In our example we use the relationships $t_b \Delta f_{\text{Mod. Costas}} = 5$ and $t_b B = 12.5$. The frequency evolution during pulse 2 is shown in Fig. 17. The LFM slope polarity alternates between bits whose frequency slots are adjacent, in order to reduce their relatively large spectral overlap [9].

With $M = 16$ elements, the normalized bandwidth is

$$t_b(f_{\max} - f_{\min}) = t_b B + (M-1) t_b \Delta f_{\text{Mod. Costas}} = 12.5 + 15 \cdot 5 = 87.5 \quad (6)$$

and the single-pulse time-bandwidth product (TBW) is

$$T(f_{\max} - f_{\min}) = M t_b (f_{\max} - f_{\min}) = 16 \cdot 87.5 = 1400. \quad (7)$$

Recall that the product of the bit duration times the overlay frequency step is only $t_b \Delta f = \pm 0.25$, which is very small compared with the minimal modified Costas normalized frequency step of $t_b \Delta f_{\text{Mod. Costas}} = 5$. Thus the frequency evolution of the other 7 pulses in the train will be very similar to that of the 2nd pulse, plotted in Fig. 17.

The ACF of the modified Costas pulse with DP overlay is shown in Fig. 18 using three zooms. The removal (below -70 dB) of the near sidelobes occurs beyond $\tau = 2t_b = t_s$. The remaining sidelobes, below $\tau = 2t_b = t_s$, are lower than -35 dB. The peak level of the first recurrent lobe is approximately -20 dB. The ACF mainlobe width is approximately $0.012 t_b \approx T/1300$, which agrees quite well with the TBW product in (7).

The ambiguity function is shown in Fig. 19. The delay axis extends over ± 6 bits which is 3/8th of a pulsewidth. The Doppler axis extends as far as $\nu = 5/(PT_r) = 5/(8T_r)$. Except for the Doppler axis (where the ambiguity function is independent of any FM), the ambiguity function exhibits a relatively uniform, very low pedestal.

VI. CONCLUSIONS

We showed that in a coherent train of pulses, practically the same ACF sidelobes removal can be achieved when implementing orthogonal overlay using DP, which is frequency coding, rather than the original binary phase-coded overlay. The added frequency coding is especially attractive for signals in which the pulse compression was obtained originally through FM. The DP overlay was demonstrated on four types of pulse train signals: unmodulated pulses, Costas pulses, LFM pulses, and modified Costas pulses. Orthogonal overlay using DP produced complete removal of almost the same portion of the near sidelobes, as did phase-coded overlay. It also drastically attenuated (below -20 dB) the recurrent lobes. Finally, its spectrum decayed faster than when phase-coded overlay was used.

NADAV LEVANON
Electrical Engineering Systems
Tel Aviv University
PO Box 39040
Tel Aviv 69978
Israel
E-mail: (nadav@eng.tau.ac.il)

REFERENCES

[1] Mozeson, E., and Levanon, N.
Removing autocorrelation sidelobes by overlaying orthogonal coding on any train of identical pulses.
IEEE Transactions on Aerospace and Electronic Systems, **39**, 2 (2003), 583–603.

[2] Levanon, N., and Mozeson, E.
Orthogonal train of modified Costas pulses.
Proceedings of the IEEE 2004 Radar Conference, Philadelphia, PA, Apr. 2004, 255–259.

[3] Levanon, N., and Mozeson, E.
Radar Signals.
New York: Wiley, 2004, ch. 9.

[4] Ashe, J. M., Nevin, R. L., Murrow, D. J., Urkowitz, H., Bucci, N. J., and Nesper, J. D.
Range sidelobe suppression of expanded/compressed pulses with droop.
Proceedings of the 1994 IEEE National Radar Conference, Atlanta, GA, Mar. 1994, 116–122.

[5] Faust, H. H., Connoly, B., Firestone, T. M., Chen, R. C., Cantrell, B. H., and Mokole, E. L.
A spectrally clean transmitting system for solid-state phased-array radars.
Proceedings of the IEEE 2004 Radar Conference, Philadelphia, PA, Apr. 2004, 140–144.

[6] Zulch, P., Wicks, M., Moran, B., Surova, S., and Byrens, J.
A new complementary waveform technique for radar signals.
Proceedings of the IEEE 2002 International Radar Conference, Long Beach, CA, Apr. 2002, 34–40.

[7] Proakis, J. G., and Salehi, M.
Communication Systems Engineering (2nd ed.).
Upper Saddle River, NJ: Prentice Hall, 2002, ch. 10.

[8] Costas, J. P.
A study of a class of detection waveforms having nearly ideal range-Doppler ambiguity properties.
Proceedings of the IEEE, **72**, 8 (1984), 996–1009.

[9] Levanon, N., and Mozeson, E.
Modified Costas signal.
IEEE Transaction on Aerospace and Electronic Systems, **40**, 3 (2004), 946–953.